Science of the Total Environment 831 (2022) 154772

Contents lists available at ScienceDirect

Science of the Total Environment

journal homepage: www.elsevier.com/locate/scitotenv

Leaching material from Antarctic seaweeds and penguin guano affects cloud-relevant aerosol production

Manuel Dall'Osto [a,*], Ana Sotomayor-Garcia [a], Miguel Cabrera-Brufau [a], Elisa Berdalet [a], Dolors Vaqué [a], Sebastian Zeppenfeld [b], Manuela van Pinxteren [b], Hartmut Herrmann [b], Heike Wex [c], Matteo Rinaldi [d], Marco Paglione [d], David Beddows [e], Roy Harrison [e,1], Conxita Avila [f], Rafael P. Martin-Martin [f], Jiyeon Park [g], Andrés Barbosa [h]

[a] Department of Marine Biology and Oceanography, Institute of Marine Sciences (CSIC), Pg. Marítim de la Barceloneta, 37-49, E-08003 Barcelona, Catalonia, Spain
[b] Atmospheric Chemistry Department (ACD), Leibniz-Institute for Tropospheric Research (TROPOS), D-04318 Leipzig, Germany
[c] Experimental Aerosol and Cloud Microphysics Department, Leibniz-Institute for Tropospheric Research (TROPOS), D-04318 Leipzig, Germany
[d] National Research Council, Institute of Atmospheric Sciences and Climate, Bologna, Italy
[e] National Centre for Atmospheric Science Division of Environmental Health & Risk Management School of Geography, Earth & Environmental Sciences University of Birmingham, Edgbaston, Birmingham B15 2TT, UK
[f] Department of Evolutionary Biology, Ecology, and Environmental Sciences, University of Barcelona & Biodiversity Research Institute (IRBio), Av. Diagonal 643, 08028 Barcelona, Catalonia, Spain
[g] Korea Polar Research Institute, 26 Songdomirae-ro, Yeonsu-gu, Incheon 21990, South Korea
[h] Departamento de Ecología Evolutiva, Museo Nacional de Ciencias Naturales, CSIC, C/José Gutiérrez Abascal, 2, 28006 Madrid, Spain

HIGHLIGHTS

- We conducted sea spray aerosol (SSA) chamber experiments in Antarctic coastal systems.
- We studied the effect of leachate material from macroalgae and penguin guano on SSA production.
- The addition of different leachate materials affects SSA production.
- Marine organic matter in the surface ocean biogeochemistry should be considered in global climate models.

GRAPHICAL ABSTRACT

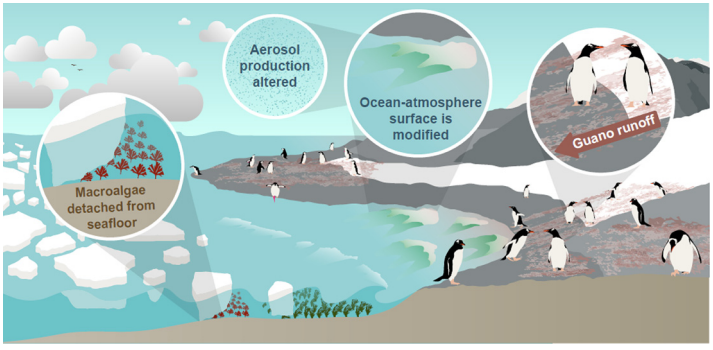

ARTICLE INFO

Article history:
Received 13 December 2021
Received in revised form 12 March 2022
Accepted 19 March 2022
Available online 29 March 2022

Editor: Pingqing FuEditor: Pingqing Fu

Keywords:
Sea spray aerosols

ABSTRACT

Within the Southern Ocean, the greatest warming is occurring on the Antarctic Peninsula (AP) where clear cryospheric and biological consequences are being observed. Antarctic coastal systems harbour a high diversity of marine and terrestrial ecosystems heavily influenced by Antarctic seaweeds (benthonic macroalgae) and bird colonies (mainly penguins). Primary sea spray aerosols (SSA) formed by the outburst of bubbles via the sea-surface microlayer depend on the organic composition of the sea water surface. In order to gain insight into the influence of ocean biology and biogeochemistry on atmospheric aerosol, we performed in situ laboratory aerosol bubble chamber experiments to study the effect of different leachates of biogenic material - obtained from common Antarctic seaweeds as well as penguin guano - on primary SSA. The addition of different leachate materials on a seawater sample showed a dichotomous effect depending on the leachate material added - either suppressing (up to 52%) or enhancing (22–88%) aerosol particle

* Corresponding author.
E-mail address: dallosto@icm.csic.es (M. Dall'Osto).
[1] Also at: Department of Environmental Sciences/Center of Excellence in Environmental Studies, King Abdulaziz University, PO Box 80203, Jeddah, 21589, Saudi Arabia.

http://dx.doi.org/10.1016/j.scitotenv.2022.154772

Antarctic
Sea ice-atmospheric interactions
Atmospheric marine biogeochemistry
CATCH
BEPSII
SOLAS

production. We found high ice nucleating particle number concentrations resulting from addition of guano leachate material. Given the evolution of upper marine polar coastal ecosystems in the AP, further studies on ocean-atmosphere coupling are needed in order to represent the currently poorly understood climate feedback processes.

1. Introduction

Aerosols in the atmosphere play a critical role in the climate system - they interact with incoming solar radiation and they can act as cloud condensation nuclei (CCN) and ice nucleation particles (INP) (Carslaw et al., 2013). Currently, aerosol-cloud interactions are not fully understood, and related uncertainties propagate errors in model representations of climate feedback processes (Stocker et al., 2013). A major uncertainty comes from the lack of understanding of aerosol sources and their dynamics, especially in the remote marine atmosphere. Several studies points to primary sea spray aerosols (SSA) contributing to the aerosol particle mass and number concentrations. These are in contrast the hypothesis of climate regulation via emissions of dimethyl sulphide marine biogenic emissions forming new particles (Quinn et al., 2015; Quinn and Bates, 2011; Brean et al., 2021). This is particularly true in the Southern Ocean, one of the most pristine regions on Earth (Chubb et al., 2016; Fossum et al., 2017). Despite a three-decades long debate (Quinn and Bates, 2011; Fossum et al., 2017), processes linking marine biota, marine aerosols, and cloud droplet number concentrations are still not well understood.

Sea spray aerosols (SSA) are atmospheric primary marine aerosols coming from the interaction between oceanic waves and the generated bubble busting in the sea surface (Gantt and Meskhidze, 2013; Quinn et al., 2015). The surface of the ocean - the source of sea spray aerosols - contains a vast amount of microorganisms, whose activity greatly contributes to the bulk of organic matter (OM) containing carbon mainly divided into dissolved organic carbon (DOC) and particulate organic carbon (POC) (Cunliffe et al., 2013; Vaqué et al., 2021). OM can greatly affect the hygroscopic properties and CCN activity of aerosols, but the mechanism and extent to which marine biogeochemistry activities affect atmospheric aerosol properties remain controversial (Quinn et al., 2015; Mansour et al., 2020; Lewis et al., 2021). It is imperative to understand the biogeochemical processes that produce OM in ocean surface waters in order to fully understand the ocean-atmosphere relationships.

The Southern Ocean has complex interconnected environmental components – such as ocean circulation, sea ice formation and melting, and land and snow variable coverage – which are very sensitive to climate change. Within the Antarctic continent, the peculiar Antarctic Peninsula has been experiencing some of the fastest warming winters on the planet since observations began in the 1950s. Rapid climatic changes affecting atmospheric/ocean circulation, ocean properties and sea ice covering are altering marine ecosystems as well. Indeed, field data collected at the AP suggest that regional ecosystems and relative biogeochemical cycles are shifting. How polar marine ecosystems respond to rapid climate change in the AP was reviewed by Schofield et al. (2017). Briefly, large phytoplankton blooms support rich marine ecosystems; the intensity of such blooms have declined about 10% over the last three decades. There is evidence that the phytoplankton community composition has shifted from large to small cells and such changes are not geographically uniform (Moran et al., 2010; Convey and Peck, 2019). The observed shifts in phytoplankton biomass and size also impact the grazer communities, especially Antarctic krill and salps. Given there is a link between phytoplankton primary producers and consumers populating the upper oceanic levels, the shift of the zooplankton communities have an impact also on the higher trophic levels such as penguins and other bigger animals (seals, whales).

Within the present study, we focus on the organic material leached from seaweeds and penguin guano material. We choose these two leaching material sources due to the evidence that the potential impact of Antarctic coastal ecosystems on aerosol composition has been overlooked in past studies (Decesari et al., 2020; Rinaldi et al., 2020). The sea-surface microlayer (SML) - a <1 mm layer at the air-sea boundary, and spontaneously emerging surface phenomena, such foams - patches floating on the water surface (Wong et al., 2021; Rahlff et al., 2021) - are found increasing research interest (Wurl et al., 2017; Engel et al., 2017). The main objective of this work is to test whether organic leaching material from ecologically rich coastal ecosystems has an effect on sea spray aerosol production in the sensitive area of the AP.

We therefore briefly discuss Antarctic coastal polar marine ecosystems influenced by seaweed and penguin habitats. In Antarctica, the coastline extends for 17,968 km and comprises about 34.8–36.4 $\times$ 10^6 km^2 of ocean surface where 80% of this is covered by ice, even in summer (Ronowicz et al., 2019). Overall, there are about 390,071 km^2 of free ice coast shallower than 200 m (Peck, 2018). Antarctic seaweeds (often called macroalgae) populate Antarctic coastal areas that are shallow (<200 m), rocky shores can cover more than 80% of the benthic surface (Amsler et al., 2005; Wiencke and Amsler, 2012). They comprise a large group of diverse eukaryotic, photosynthetic and macroscopic marine organisms (Gómez et al., 2009; Gómez and Huovinen, 2020; Pellizzari et al., 2017; Rovelli et al., 2019; Wiencke et al., 2002, Lagger et al., 2018; Quartino et al., 2013, 2020). Seaweeds dominate in terms of biomass the benthic areas where hard substratum, like rocky formations or cobbled bottoms, is available (Fraser et al., 2020; Oliveira et al., 2020), with communities ranging from the lower parts of the photic zone (30–40 m depth) up to the intertidal areas of the shores (Campana et al., 2020), and contributing substantially to nearshore food webs and local benthic ecology (Ankisetty et al., 2004; Corbisier et al., 2004; Quartino et al., 2005; Iken et al., 2009). While macroalgae can be found in all the Antarctic continent, the largest and most diverse abundance is found the region West of the AP (Wiencke and Clayton, 2002; Amsler et al., 2005). The biomass of these seaweeds has been estimated as between 1.5 and 10 kg m^{-2} wet weight (Gómez et al., 2009; Wiencke and Amsler, 2012), being comparable to temperate kelp forests. Furthermore, ice scouring and weather – e.g., seastorms - can produce large events of seaweed detachment. In these situations, algal fragments can accumulate in huge amounts in seabed hollows and coastlines, where they are grazed upon by herbivores or degraded by microbes, contributing to carbon dynamics (Clarke et al., 2007; Clark et al., 2015, 2017).

Seabirds are important indicators of ecosystem status and are among the species impacted by climate change. Seabirds are one of the more abundant vertebrates in the Southern Ocean living during several months in breeding colonies of up to several thousands of pairs (Garcia-Borboroglu and Boersma, 2013), and being important global drivers in the nitrogen and phosphorus cycles (Otero et al., 2018). Half of the total seabird populations are distributed in the Antarctic and Sub-Antarctic region (Otero et al., 2018). Penguins represent a high proportion of the avian biomass (Boersma, 2008) and they are a significant source of atmospheric ammonia (NH_3) through their fecal excretion (known as "guano") in remote Antarctic systems. This is an important source of nitrogen that enhances vegetable growth and has an impact on both terrestrial and marine ecosystems (Zhu et al., 2014). This fecal material contains high concentrations of macro and micronutrients and is one of the main source of P and N representing around 80% of the amount of these elements in the Antarctic marine environment (Otero et al., 2018). On the other hand, seabird colonies are responsible for severe environmental changes at the regional level in soils (Abakumova et al., 2021) and affect the magnitude of the N and the P fluxes associated with ornitheutrophication, which is comparable with other processes considered in biogeochemical global inventories (Otero et al., 2018).

To our knowledge there are no studies investigating the effect of Antarctic leaching material derived from macroalgae and penguin fecal material on primary SSA production. To shed light on this question, we conducted experiments using an aerosol bubble bursting chamber to generate primary

sea spray marine aerosols from seawater samples. This experimental setup is commonly used in ocean-atmosphere biogeoscience studies to produce SSA comparable to oceanic aerosols (Fuentes et al., 2010; Sellegri et al., 2021; Cochran et al., 2017; Prather et al., 2013). Our studies show a complex relationship between the biogeochemical properties of different waters and the relative primary sea spray produced. Our multidisciplinary ocean-atmosphere study contributes to an understanding of the response of the AP ecosystems to climate change.

2. Methodology

2.1. Location and sampling

The experiments were performed at the Spanish Antarctic Base (BAE JC1) research station in Livingston Island (62.66° S, 60.39° W). We collected seawater (SW21) from Johnson Bay - next to the BAE - the same seawater was used as a common seawater matrix to run all the leaching experiments. Guano material was collected in a glacier pond on land next to a penguin colony and maintained frozen at −20 °C. Three different Antarctic seaweeds, among the main species found in the South Shetland Islands (Gallardo et al., 1999; Amsler et al., 2005), were collected on Livingston Island beach near the BAE: the red alga *Palmaria decipiens*, the brown algae *Desmarestia antarctica* and the brown algae *Desmarestia menziesii* (Table S1).

In term of biomass, the Rhodophyte *Palmaria decipiens* is the most abundant species in the Antarctic costal continent as well as the Antarctic islands. It is reported as the predominant macroalgae covering the bays and the coves of the AP; it is found below the ocean at a depth between about zero and seventy metres although the majority of the mass is found between zero and thirty metres due to light needs (Gómez et al., 2009).

Palmaria decipiens has been described to contain diverse polysaccharides, including xylose, galactose and traces of glucose, as well as an acidic polysaccharide composed by galactose, xylose, galacturonic and glucuronic acids, probably conforming an acidic xylogalactan-protein complex (Matsuhiro and Urzúa, 1996). *P. decipiens* also contains a range of UV-absorbing pigments that change along its annual growth cycle, with maximum concentrations and complexity of the Microsporine Amino Acids (MAA) occurring in the mature fronds in the Summer (Carreto et al., 2005). Several carotenoids have been also described in *P. decipiens*, conforming to a simple carotenoid pattern (Marquardt and Hanelt, 2004). Regarding brown seaweeds, we analyzed *Desmarestia menziesii* and *Desmarestia antarctica* (Amsler et al., 2005, 2008; Benites Guardia, 2019; Dos Santos et al., 2020; Iken et al., 2011). They both may release sulphuric compounds when damaged or exposed to changing environmental conditions (e.g., when they are preyed upon by herbivores or individuals are broken and beached on the intertidal areas by sea storms), which destroys their own tissues and can have extensive effects on the surrounding organisms (Gagnon et al., 2006, 2012; Pelletreau and Muller-Parker, 2002). The three macroalgae samples (Table S1) were placed in 200 L containers with seawater (also from Johnson Bay) for two weeks exposed to the natural light and ambient temperature conditions. This period allowed their progressive degradation and the leached organic material was then used in the experiments. The four different leaching material samples are summarized in Table S2. The samples were filtered via a 100 μm filter before each experiment.

Our study - to our knowledge - is the first one analyzing the effect of different Antarctic organic material leached on the surface ocean and affecting SSA production in Antarctica. We consider this a pilot study, it is imperative to understand how different organic material in Antarctica may affect the sea spray production. Given most SSA studies always take the Chl-*a* as referent organic material (Rinaldi et a., 2013), the original water (SW21, Chl-*a* 1.5 μg m^{-3}) and the waters with the leached material (SW 22–25, Chl-*a* 1.5 ± 1 μg m^{-3}) had the same order of magnitude. The average Chl-*a* concentration in seawater samples collected nearby were in the order of about 0.04–6 μg L^{-1} (Zeppenfeld et al., 2020), our laboratory experiments have Chl-*a* values in the order with the literature.

2.2. Aerosol generation chamber and experiments design

Bubble-bursting sea spray aerosol (SSA) generation experiments were performed in a stainless steel 70 L tank. The "OLLA" aerosol primary chamber is a tank of 55 cm height by 44 cm diameter, this allow to use high volumes of waters (about 70 L) that are necessary to research different chemical and biological parameters (Park et al., 2019, 2020; Medina-Pérez et al., 2020). The water goes around via a teflon tube from the bottom to the top of the tank via a peristaltic pump (flow rate 12 L min^{-1}): a plunging jet over the surface of the water entrain air and form bubbles. These produce SSA via bubble bursting. Compressed air is blown into the free water headspace (about 70 L) at about 60 L min^{-1}. The aerosol chamber was washed and cleaned with milliQ water after each experiment. Outlet ports sampled the SSA particle size distributions using a Scanning Mobility Particle Sizer (SMPS; DMA TSI 3080 and CPC TSI 3025, corrected for diffusion losses). Number size distributions of the aerosol, across the 10–500 nm size range, were collected using the SMPS with scan times of 5 min.

2.3. Biological and chemical parameters estimated in the seawater

Seawater samples collected before the aerosol generation period were kept frozen until the analyses conducted at the laboratories within six months after collection; only Chl-*a* were run fresh in the BAE laboratory.

2.3.1. Virus and prokaryote abundance

Subsamples (2 mL) for virus and prokaryote (bacteria and archaea) abundances were fixed with glutaraldehyde (0.5% final concentration) and stored at −80 °C. Counts were made on a FACSCalibur (Becton & Dickinson, Franklin Lakes, NJ, USA) flow cytometer in the ICM-CSIC laboratory. Virus samples were diluted with TE-buffer (10:1 mM Tris:EDTA), stained with SYBR Green I, and run at a medium flow speed (Brussaard, 2004), with a flow rate of 58–64 μL min^{-1}. Different groups of viruses (VA) were determined in bivariate scatter plots of green fluorescence of stained nucleic acids versus side scatter (Evans et al., 2009). Depending on their fluorescent signal, viruses were classified as low (V1), medium (V2) or high (V3 and V4) fluorescence that correspond to their DNA content. It is presumed that, fractions V1 and V2 are mainly attributed to bacteriophages, and V3 and V4 to viruses of eukaryotes (Evans et al., 2009). Prokaryote abundance (PA) samples were stained with SYTO13 (SYTOTM13, ThermoFisher) and counted following the protocol of Gasol and Del Giorgio (2000), and high DNA and low DNA content was discerned.

2.3.2. Nanoflagellate abundance and biomass

Nanoflagellate abundance was estimated on seawater subsamples (15–20 mL) fixed with glutaraldehyde (1% final concentration). After ca. 1 h fixation at 4 °C, the samples were filtered through 0.6 μm black polycarbonate filters, and stained with 4,6-diamidino-2-phenylindole (DAPI) at a final concentration of 5 μg mL^{-1} (Sieracki et al., 1985). The filters were mounted on porta-slides, with immersion oil, and frozen at −20 °C until observation at the ICM-CSIC. Cell counts were conducted by epifluorescence microscopy (Olympus BX40–102/E at 1000×), with blue wavelength excitation (BP 460–490 nm) and barrier (BA 510–550 nm) filters, and an ultraviolet excitation (BP 360–370 nm) and barrier (BA 420–460 nm) filters. Cell counts were conducted on three transects per 5 mm of each collected filter.

Phototrophic nanoflagellates (PNF) could be distinguished from heterotrophic nanoflagellates (HNF), based on red fluorescence emission by plastidic structures upon blue light excitation. When possible, identification at the taxa was conducted at genus or order level. HNF and PNF cell size measures were conducted and four size classes were established (≤2 μm, 2–5 μm, 5–10 μm and 10–20 μm) with an inferred average radius (considering cells as spheres) of 0.75 μm, 1.5 μm, 3 μm and 6 μm, respectively. The contribution of HNF and PNF to the carbon biomass (μg C L^{-1}) was estimated by the corresponding carbon-volume ratio, namely, pgC $cell^{-1}$ = 0.216* $(V)^{\hat{}0.939}$ described in Mender-Deuer and Lessard (2000).

2.3.3. Phytoplankton identification, abundance and biomass

Seawater samples (100 mL) were collected in amber glass bottles, fixed with hexamine buffered formalin (4% final concentration) and preserved dark at 4 °C for quantification of phytoplankton taxa using the Utermöhl (1931, 1958) method as described for instance by Edler and Elbrächter (2005). Samples were gently shaken and poured into 50 mL methacrylate cylinders of settling chambers. After sedimentation for 24 h, samples were counted using an inverted XSB-1A microscope equipped with 4, 10, 25 and 40× flat optics objectives and 10× eyepieces with a 1.25× intermediate lens. The entire base of the settling chambers was scanned at 125× magnification to quantify the organisms which were less abundant and of larger size of the microphytoplankton (>20 μm), and transects (2 minimum) conducted at 312× magnification to quantify the most abundant organisms and nanoplankton (<20 μm). The identification was made at the most precise possible species or genus level. Phytoplankton results are expressed in number of cells per liter. Empty cells were not considered in this study.

For each taxon, its contribution to particulate carbon was calculated from biovolume measures following Mender-Deuer and Lessard (2000). Cell dimensions (length, width and thickness, in μm) estimations were performed using a digital camera and Scope Photo software, calibrated according to the microscope used. For each identified species, cell volume was calculated from average length and width values using the formula of the closest geometric figures approximation. Setae and expansions (horns, wings, etc.) dimensions were excluded; in the case of the flattened organisms, manual corrections of the thickness were applied.

2.3.4. Chlorophyll a

For Chl-*a* concentration estimation, 100 mL of seawater were filtered through a 25 mm diameter GF/F glass fiber filter (Whatman). The contribution of the nanophytoplankton was determined by collecting the seawater in the GF/F filters after a previous filtration through 5 μm Millipore polycarbonate filters. Chl-*a* was extracted in 90% acetone for 24 h in the dark at 4 °C. Concentrations were determined by fluorimetry with a calibrated Turner Designs fluorometer following the method developed by Holm-Hansen et al. (1965).

2.3.5. Inorganic and organic nutrients

Dissolved inorganic nutrients (nitrate, phosphate and silicate) were measured with standard segmented flow analysis with colorimetric detection, using a SEAL Auto Analyzer AA3 HR (BBMO) or Bran + Luebe autoanalyzer (EOS).

2.3.6. DOC

For dissolved organic carbon (DOC) analysis 30 mL of seawater were filtered through precombusted (450 °C, 24 h) 47 mm GF/F glass fiber filters (Whatman), in a filtration system under controlled pressure conditions with nitrogen gas. The filter was prewashed with milliQ water, and the collecting flask was rinsed three times with filtered sample water before use. The sample was stored frozen (−20 °C) until analysis in the laboratory. Following the elimination of inorganic carbon by the acidification of the sample, determination of DOC in seawater was conducted by high temperature catalytic oxidation (680 °C) as described in Álvarez-Salgado and Miller, 1998. Measurements were conducted with the TOC-V CSH Shimadzu autoanalyzer that holds a NDIR (non-dispersive infrared) detector using Milli-Q water as a blank, potassium hydrogen phthalate as the calibration standard, and deep Sargasso Sea water as the reference (Hansell Laboratory. University of Miami, RSMAS). Concentrations are expressed as μmol C L^{-1}.

2.3.7. CDOM

Samples for coloured dissolved organic matter (CDOM) characterization were filtered in the same manner as those of DOC and immediately analyzed using a Horiba Aqualog spectrofluorometer.

2.3.8. POC

For POC analysis, seawater samples (1000 mL) were filtered through precombusted (4 h, 450 °C) 25 mm GF/F glass fiber filters (Whatman) which were immediately frozen at −80 °C and subsequently maintained at −20 °C until further processing. Filters were dried and analyzed with an elemental analyzer (Perkin-Elmer 2400 CHN). Concentrations are expressed as μmol C L^{-1}.

2.3.9. TEP and CSP

Samples for determination of the concentration of Transparent Exopolymer (TEP) and Coomassie Stainable Particles (CSP) were collected in triplicate by very gentle filtration (~150 mmHg vacuum) on 25 mm diameter 0.4 μm pore size polycarbonate filters (DHI). TEP concentration was determined following the colorimetric method described by Passow and Alldredge (1995) and the analogous method developed by Cisternas-Novoa et al. in 2014 was followed for the CSP. For TEP determination, filters were stained with an Alcian Blue (8GX) solution (500 μL, 0.02%, pH 2.5) for 5 s. CSP filters were stained with 1 mL of Coomassie Brilliant Blue (CBB-G 250) solution (0.04%) for 30 s, prepared daily with filtered (0.2 μm) seawater. Immediately after staining, all filters were rinsed with milli-Q water and stored in 2 mL micro-vials at −20 °C. Triplicate blanks (empty filters) were stained daily for TEP and for CSP with the corresponding staining method used for regular samples. Sample dye extraction and measurements of absorbance were performed in the ICM-CSIC using a Varian Cary 100 Bio spectrophotometer. Both staining solutions were calibrated following their respective methods. TEP staining solution was calibrated before and after the PI-ICE cruise using xanthan gum (XG) as a standard. CSP staining solution was calibrated using bovine serum albumin (BSA) after the cruise to consider salinity. Accordingly, TEP concentrations are expressed as xanthan gum equivalents (μg XG equiv. L^{-1}) and CSP concentrations as BSA equivalents (μg BSA equiv. L^{-1}).

2.4. Dissolved and particulate carbohydrates in seawater

Dissolved free carbohydrates (DFCHO), dissolved combined carbohydrates (DCCHO, <0.2 μm) and particulate combined carbohydrates (PCCHO, >0.2 μm) were determined as described by Zeppenfeld et al. (2020, 2021). For the analysis of DFCHO and DCCHO, a filtered subsample of 9 mL (0.2 μm Millex syringe filter) was desalinated by electro-dialysis. For PCCHO, 50–100 mL of untreated subsample was filtered onto a 0.2 μm polycarbonate membrane filter (Ø 47 mm). DCCHO and PCCHO were determined after an acid hydrolysis (0.8 M HCl, 100 °C, 20 h) of a filtered, desalinated aliquot or a weighed piece of the air-dried membrane filter, respectively. DFCHO, DCCHO and PCCHO were calculated as the sums of the monosaccharides, which could be determined with high-performance anion-exchange chromatography with pulsed amperometric detection (HPAEC-PAD) equipped with a Dionex CarboPac PA20 analytical (3 mm × 150 mm) and guard column: these were fucose, rhamnose, arabinose, galactose, glucose, xylose, mannose, fructose, galactosamine, glucosamine, muramic acid, galacturonic acid, glucuronic acid. All samples were measured in duplicate.

2.5. Ice nucleating particles (INP)

Number concentrations of INP were determined using two well established freezing essays, described in detail in Gong et al. (2020) and Hartmann et al. (2021). Either 90 or 96 droplets with volumes of either 1 or 50 μL were pipetted onto hydrophobic glass slides or into PCR-trays for these two methods, namely LINA (Leipzig Ice Nucleation Array) or INDA (Ice Nucleation Droplet Array), respectively. The hydrophobic glass plates were then cooled down on the Peltier element of a cold stage in LINA, and the PCR-trays used in INDA were cooled down in a thermostat operated with ethanol. The number of frozen droplets was determined automatically from pictures taken during the cooling process, on which the change from a liquid to a frozen droplet can clearly be seen in a change of the reflectivity, and hence of the grey value, of the droplets. From the obtained cumulative count then INP concentrations per volume of sample were determined in a

way usually used for this kind of measurements, using Poisson statistics as suggested by Vali (1971).

2.6. ^{1}H NMR spectroscopy analysis

Quartz-fiber filter were used to collect Particulate Organic Carbon (POC). The filters from the bubble bursting experiments were then extracted with Milli-Q (deionized ultra pure water) by meaning of mechanical shaking (1 h). The suspended particles were removed by filtration (PTFE membranes, pore size: 0.45 μm). As explained in Decesari et al. (2020), the extracts were dried under vacuum and dissolved again in deuterium oxide (D2O) for the characterization of the organic groups by using ^{1}H NMR spectroscopy. We recorded the ^{1}H NMR spectra with a Varian Unity INOVA (University of Bologna). The internal standard used is Sodium 3-trimethylsilyl-(2,2,3,3-d4) propionate (50 μL of a 0.05% TSP-d4 - by weight in D2O). To avoid the shifting of pH-sensitive signals, the extracts were buffered to pH about 3 using a deuterated formate/formic-acid (DCOO-/HCOOH) buffer prior to the analysis. The speciation of hydrogen atoms bound to carbon atoms can be provided by ^{1}H NMR spectroscopy in protic solvents. On the basis of the range of frequency shifts (expressed as ppm), the signals can be attributed to H-C containing specific functionalities (Decesari et al., 2000, 2020): Ar-H (6.5–8.5 ppm), aromatic protons; O-CH-O (5–6 ppm), anomeric and/or vinyl protons; H-C-O (3.2–4.5 ppm), protons bound to oxygenated aliphatic carbon atoms (hydroxyl and alkoxy groups): aliphatic alcohols, ethers, and esters; H-C-C = (1.8–3.2 ppm), protons bound to aliphatic carbon atoms adjacent to unsaturated groups like alkenes (allylic protons), carbonyl or imino groups (heteroallylic protons) or aromatic rings (benzylic protons); H-C (0.9–1.8 ppm), unfunctionalized alkylic protons.

3. Results and discussion

3.1. Primary aerosol chamber and Atmospheric aerosol measurements

The particle number concentrations and the SSA size distributions of the generated aerosols from five different experiments were measured at 15 ± 10% Relative Humidity (RH) and are reported in Fig. 1a–b (dN/dlogdp, where dp is particle mobility diameter). The size resolved particle size distributions were taken every 5 min, the averages presented in Fig. 1 are the averages of 24 points (2 h each experiment). When looking at the aerosol size distributions (Fig. 1b) obtained from seawater SW21 (sea water matrix) and different leaching material added (SW22-SW25), a dichotomous influence on aerosol particle production is observed relative to the original SW21. While in general there is an expected tendency of a relative increase in aerosol production with OM (SW23, SW24 and SW25 increasing by 26%, 65% and 96%, respectively), SW22 drastically reduces it by 60% (Fig. 1a). Our results imply that not all organic leaching material has a positive influence on primary sea spray aerosol production. Fig. 1b shows that the average mode of the probability density function of the particle number distribution for the original seawater SW21 is seen at about 193 nm for SSA generated using breaking waves, consistent with previous studies (Prather et al., 2013; Sellegri et al., 2021).

Our Particle Size Distributions (PSD) do not show major contributions in the smaller size range (<100 nm, Aitken mode). When the experiments

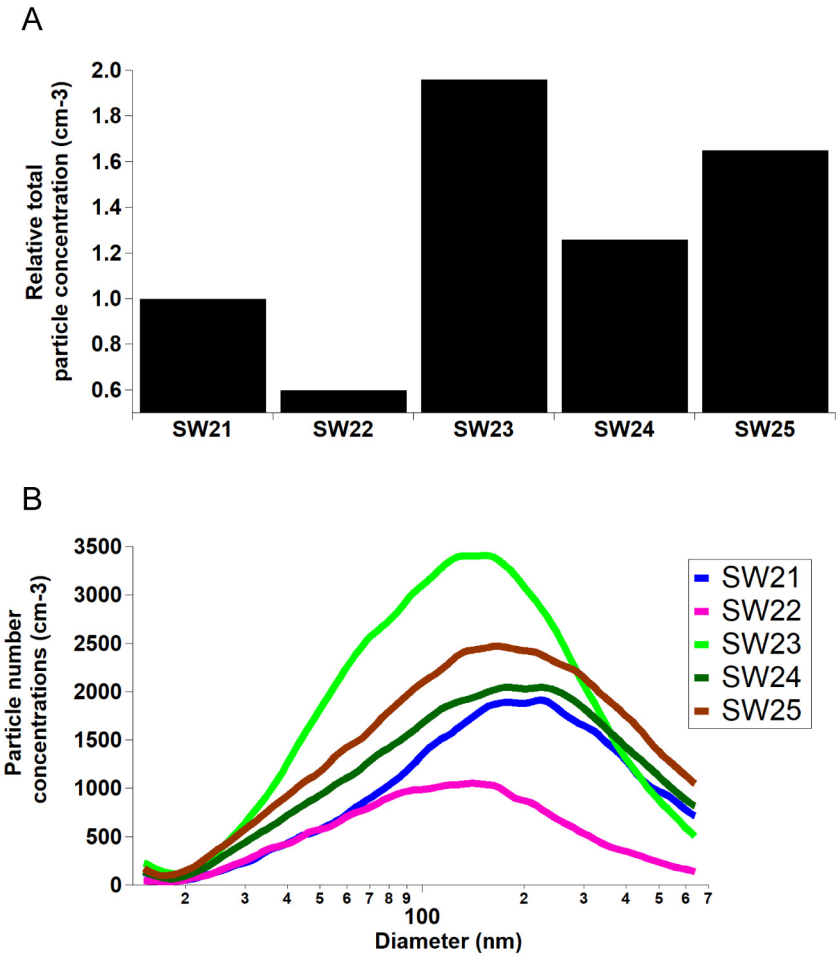

Fig. 1. a. Relative particle number concentrations (relative to the sea water matrix SW21) for the four leaching experiments. Details can be found in Table S1. Briefly, the control open water (SW21), leached material from red alga *Palmaria decipiens* (SW22), brown algae *Desmarestia antarctica* (SW23), brown algae *Desmarestia menziesii* (SW24) and penguin guano (SW25). b. Aerosol size resolved particle concentrations (cm-3) for the selected leaching material from aerosol primary chamber experiments.

are compared among each other, a clear difference in the aerosol mode is also seen. In general, adding OM reduces the aerosol average main accumulation mode diameter to 121 nm (SW22), 131 nm (SW23), 176 nm (SW24) and 176 nm (SW25).

We are aware that our study is composed only of four different organic leaching experiments. We run two additional experiments with *Palmaria decipiens* (PD 2 and PD3), during which the same amount of leached material was added to the OLLA tank, and for which only aerosol size distributions were measured. These aerosol particle size distributions revealed in both PD2 and PD3 experiments a decrease of aerosol concentration of 45% and 65%, further supporting that organic leaching material from *Palmaria decipiens* can suppress SSA production.

One remarkable result of this study addresses aerosol particles that can act as cloud condensation nuclei (CCN) at typical atmospheric cloud supersaturation (S) (Li et al., 2011). The size and chemical composition of aerosol particles determine whether they can act as CCN and hence be activated to a cloud droplet. Particle size and supersaturation have the major impacts on the activation of particles to cloud droplets. At 0.1% supersaturation (S), the largest particles with sizes above roughly 300–500 nm are likely to activate to CCN. Particles of 100–300 nm may additionally be activated at 0.2% (S), while particles of 60–80 nm typically need higher supersaturations ($\geq$0.4%) to become activated. When looking at the aerosol size distributions presented in Fig. 1b and considering only particles above 100 nm, we can see a reduction of 43% for SW22 in number, but a major increase (12–61%) for the remaining three samples. This implies that the leaching material has an impact not only on the overall size distributions but also on the abundance of particles above 100 nm, and hence on CCN on which potentially cloud droplets can form.

For the determination of INP (ice nucleating particle) number concentrations (N_{INP}), results are shown in Fig. 2. Results from the two different measurement set-ups LINA and INDA generally agree well. In general, heating, which destroys proteinaceous INP originating from microorganisms, did not cause a large change between original and heated samples for the samples shown in panels A-D. However, when comparing the guano sample in panel E with the other samples (see panel F), it is very obvious that much higher N_{INP} are observed for the guano sample in the temperature range from roughly −10 °C to −20 °C. These INP were also present in a filtered sample which was additionally examined for SW25, pointing to a size of the INP to be below 10 μm. The INP causing the ice activity in the temperature range above roughly −20 °C were completely deactivated by the heating procedure, which, as indicated above, is typically interpreted as a biogenic, proteinaceous origin of these INP. Overall, while generally low INP concentrations were found in most of our samples, there were INP found in SW25, i.e., the sample to which leaching products from guano were added. Previous INP concentrations determined during PI-ICE (Polar Interactions: Impact on Climate and Ecology field study) for both ocean and atmospheric samples were generally low (Zeppenfeld et al., 2021), in agreement with data from the Southern Ocean (McCluskey et al., 2018), and in general lower than values typically observed in the Artic (Zeppenfeld et al., 2021). The present study contributes information on possible aquatic sources of INP, where, to our knowledge, this is the first study reporting INP properties of guano and seaweeds material.

3.2. Marine sea ice microbiota

The advantage of producing and measuring extremely stable nascent SSA size distributions in a controlled laboratory setting is that it allows us to compare them with a range of biological parameters (characterizing any microorganisms such as viruses, prokaryotes -bacteria and archaea-, protists -i.e., nanoflagellates- and phytoplankton -microalgae-) (Thomas and Dieckmann, 2003). The average Chl-*a* concentration in the coastal water (SW21) was 1.5 μg L^{-1} and was significantly higher than in open water seawater samples collected nearby (about 0.04–0.4 μg L^{-1}). Three leaching material experiments presented similar Chl-*a* concentrations (Fig. 3a), about 1.5–2.0 μg L^{-1}, whereas the SW23 had higher values (2.9 μg L^{-1}). Diatoms had similar concentration levels (about 2.3 × 10^5 cell L^{-1}) in SW21-SW24, but were much higher in SW25, which was enriched with penguin defecation material (Fig. 3c). Species of the genus *Thalassiosira* were dominant in all experiments, and no major differences in diatoms groups were found among the different leaching experiments (Fig. 3c). Considering the four experiments, silicate concentrations were more than twice the inorganic nitrogen concentrations, indicating that diatoms were not limited in silicate for their frustula. Nitrate and phosphate concentrations were relatively high, suggesting that neither N nor P were limiting (Fig. S2). The high values of ammonia in SW24 may be due to possible zooplankton contamination.

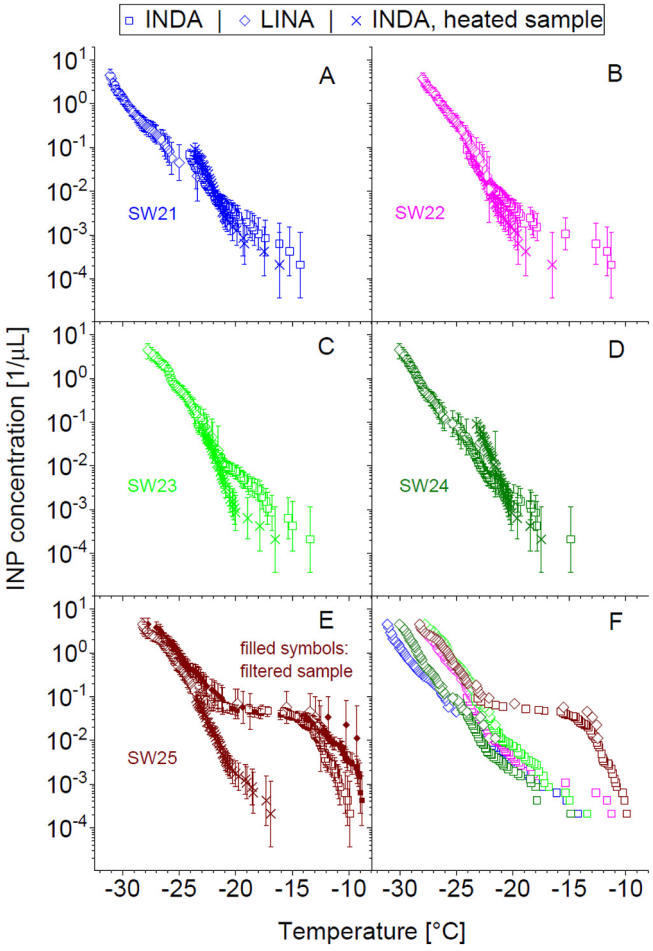

Fig. 2. INP concentrations for the described ocean-atmosphere experiments. Panels A-E show separate results for the five different samples, seawater SW21 only, *Palmaria decipiens, Desmarestia antarctica, D. menziesii*, and guano, respectively, while panel F shows all data samples combined. In each of these panels, results are shown for measurements with LINA (in the lower temperature range, due to the lower examined sample volume) and INDA (in the higher temperature range, due to the larger examined sample volume) of the original sample, and also results from INDA for samples which had been heated at 95 °C for 1 h. Panel E additionally shows data for the filtered sample.

Fig. 3F shows the total nanoflagellate (TNF) concentrations among the different experiments. Unfortunately, the water sample SW21 taken for nanoflagellate (only one) was found to be affected by contamination. Nevertheless, some differences can be seen among the different leaching material samples (SW22-SW25), where abundances reached the highest values in the brown algae leachate sample (SW23). Fig. 4 shows the prokaryote abundances and the viral abundances for the four aerosol chamber experiments. Prokaryote abundances - varying from 8 × 10^5 to 3 × 10^6 cells mL^{-1}, were found in high concentrations in the sample SW22 (*P. decipiens*) and SW23 (*D. antarctica*). Most prokaryotes had a high nucleic acid content (HNA), indicating that they were active. Broadly, HNA prokaryotes having a high content of DNA is an indication that are active cells, with a high growth rates

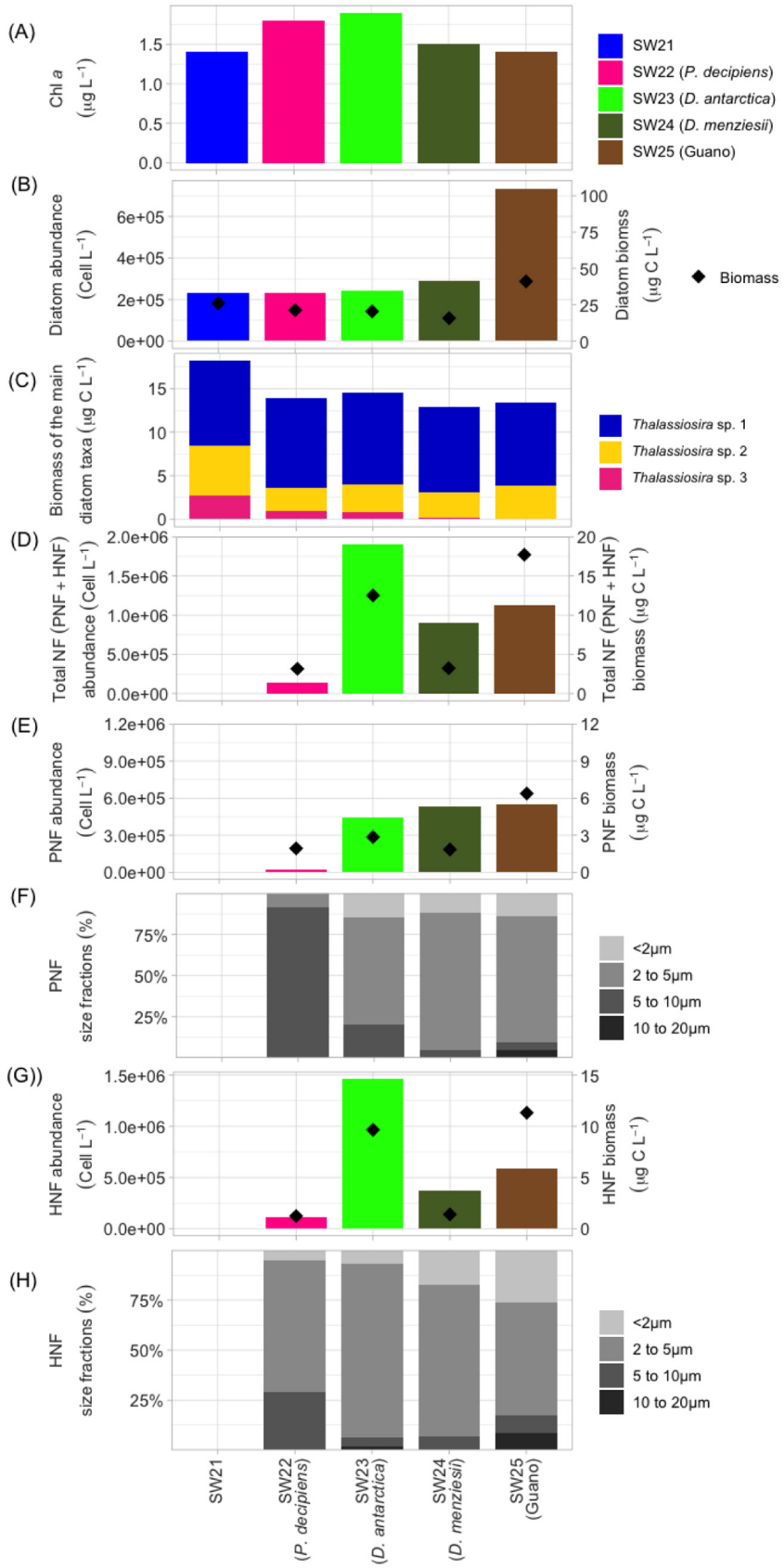

Fig. 3. Selected biological-related variables for the leaching material experiments, specifically (a) Chl-*a*, (b) diatom abundance and biomass, (c) diatom biomass main groups, (d) total nanoflagellates (TNF), (e) phototrophic nanoflagellates (PNF) abundance and biomass, (f) PNF size classes distributions, (g) heterotrophic nanoflagellates (HNF) abundance and biomass and (h) HNF size classes distributions. Data for HNF-PNF for the SW21 are not available.

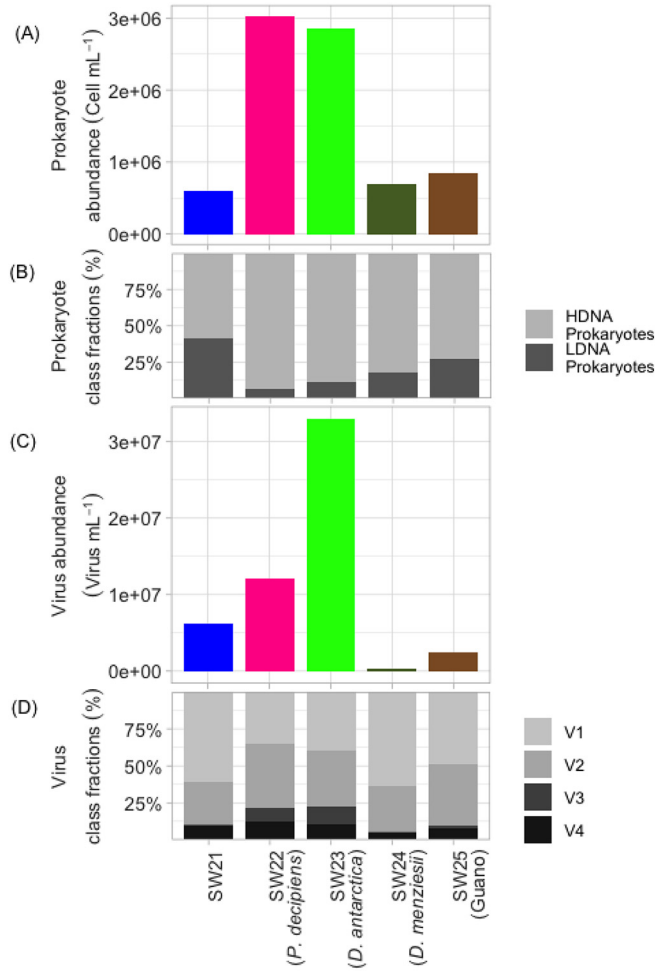

Fig. 4. Prokaryote (A–B) and Virus abundance (C–D) abundance (with relative fraction) for the PI-ICE leaching material aerosol chamber experiments.

and larger size cells than LNA prokaryotes (Gasol et al., 1999). This makes them more susceptible to be eaten by protists (HNF) or lysed by viruses for their size and activity (Vaqué et al., 2001; Bonilla-Findji et al., 2009) than LNA prokaryotes. Viral particle abundances (Fig. 4C) ranged between 2.8×10^5 viruses mL^{-1} (SW24) and 3.3×10^7 viruses mL^{-1} (SW23). The viral fractions with highest abundances were V1 and V2, corresponding mainly to bacteriophages.

3.3. Marine biogeochemical properties

3.3.1. Particulate organic carbon

Marine organic constituents occur in the ocean in dissolved and particulate form. Particulate organic carbon (POC) is defined operationally by a filtration cutoff at 0.2 to 1.0 μm. Fig. 5 shows that SW21 presents values of POC of about 11.1 μM, all measurements have higher contributions from the leaching material (35–73 μM) but by far the highest leaching contribution is associated with SW22 (430 μM). Natural organic gels - a fraction of exopolymeric substances (EPS) representing dissolved or particulate polymeric organic substances outside the cell (Engel et al., 2020) - were also measured in two major classes: polysaccharidic transparent exopolymer particles (TEP) and proteinaceous Coomassie stainable particles (CSP). Similar trends can be seen for TEP and CSP following the POC trends described above. TEP values for SW21 was 32 XG eq. μg L^{-1}, with SW 23–25 at 81–180 XG eq. μg L^{-1} and the highest was for SW22 (670 XG eq. μg L^{-1}). Similar trends were seen for CSP: for SW21 values of 55 BSA eq. μg L^{-1}, higher values for SW23–25 (55–166 BSA eq. μg L^{-1}) and the highest again for SW22 (2990 BSA eq. μg L^{-1}).

The POC extracts in the seawater show several NMR features overlapping typical biological matrices (Fig. S3). Overall, the addition of macroalgae or guano material changes substantially the sea-water POC composition enriching the water with variable amounts of amino acids and sugar-polyols of different types/quantities depending on the sample. There are common features among the samples, but they are characterized by variable content (both in term of quality and quantity) of specific compounds. In particular, the occurrence of most common aliphatic amino acids (such as alanine, threonine, valine, aspartate, glutamate, isoleucine, and leucine) was observed in all the samples analyzed and particularly in sea-water samples enriched by macroalga (SW22–24) and penguin guano (SW25).

We saw nitrogen-rich organic metabolites (Choline, Betaine, etc.) with signals by singlets (3.1–3.3 ppm) from methyl bound to nitrogen atoms (H3C-N-). We found signals due to glycerols in all our samples, and also -NCHRCO- groups of alpha-amino acids and the H-C-O groups of sugars and polyols (signals 3.4 and 4.2 ppm). Sucrose, glucose and other possible saccharides can be seen with signal of anomeric hydrogen bonds. Those were absent in the original sea-water (SW21) but are present in trace amounts in some samples (i.e., SW22 and SW25) and as major component in sample SW24 (*Desmarestia menziesii*) (Fig. S4). However, beside the overall similarity, these samples also show some differences between each other, both in the presence of specific compounds (Fig. S3) and in their relative functional group distribution (Figs. S5, S6). *Palmaria decipiens* and *Desmarestia antarctica* algae are the only ones showing H-C-O possibly of acidic sugars (e.g., uronic acids) or sulfonate-esters in the region 4.0–4.5 ppm (Fig. S3). Looking at the relative functional group distribution it is worth noting how the *P. decipiens*, as well as *Desmarestia antarctica* and *D. menziesii* (SW22, SW23 and SW24 respectively), seem to enrich the water especially with H-C-O groups of polyols and sugars. However, *P. decipiens* and *D. antarctica* are depleted both in substituted and un-substituted aliphatic chains (HCC and HC), while *D. menziesii* (SW24) has the stronger reduction only in linear HC (governed by the strong decrease of most of the already mentioned aliphatic amino acids characterizing all the other POC samples). On the other hand, *D. menziesii* shows the biggest contribution of H-C-O groups of neutral sugars (including the already mentioned sucrose and glucose) (Fig. S3). *D. antarctica* and guano show also detectable signals of low-molecular-weight alkyl amines, in particular di- and tri-methyl amine (DMA and TMA) singlets at 2.72 and 2.89 ppm, respectively. The DMA singlet is detectable also in *P. decipiens* (red algae) sample, while TMA is not. In summary, the NMR analysis (Fig. S3-S6) cannot clearly separate major differences and cannot help in describing the major differences seen in the aerosol production seen in Fig. 1.

3.3.2. Dissolved organic carbon (DOC)

DOC for SW21 was 94 μM, and higher values were seen for SW22 (5200 μM), SW23 (1340 μM), SW 24 (2580 μM), and SW25 (295 μM). All experiments with macroalgae leachate and guano (SW22–25) show much higher absorbances than that of SW21 (Fig. 6a), indicating an enrichment in coloured dissolved organic matter (CDOM) in all leached water samples. Beside the very high concentrations reported for the SW22 (likewise the POC described in Fig. 5), no clear correlations were seen when the particle number concentrations was scaled to the POC or the DOC concentrations, implying complex unknown relationships exists between the organic composition of the SSA generated and the particle production.

Several spectral features were identified in the normalized spectra of enriched samples (Fig. 6b). In SW22, enriched with decaying *Palmaria decipiens*, a broad peak centred at ~325 nm dominates the absorbance. This broad peak is most probably a combination of the absorbances of multiple mycosporine-like amino acids (MAAs), which have been reported to be produced by this species in very high concentrations as a photoprotective strategy. Specifically, MAAs shinorine (334 nm), porphyra 334 (334 nm), palythine (319 nm) and asterina 330 (330 nm) are induced in *P. decipiens* by exposure to UV radiation. SW23 and SW24, both enriched with Brown macroalgae, show very similar spectral shapes despite of the much lower total absorbance of SW23. These samples present a characteristic shoulder

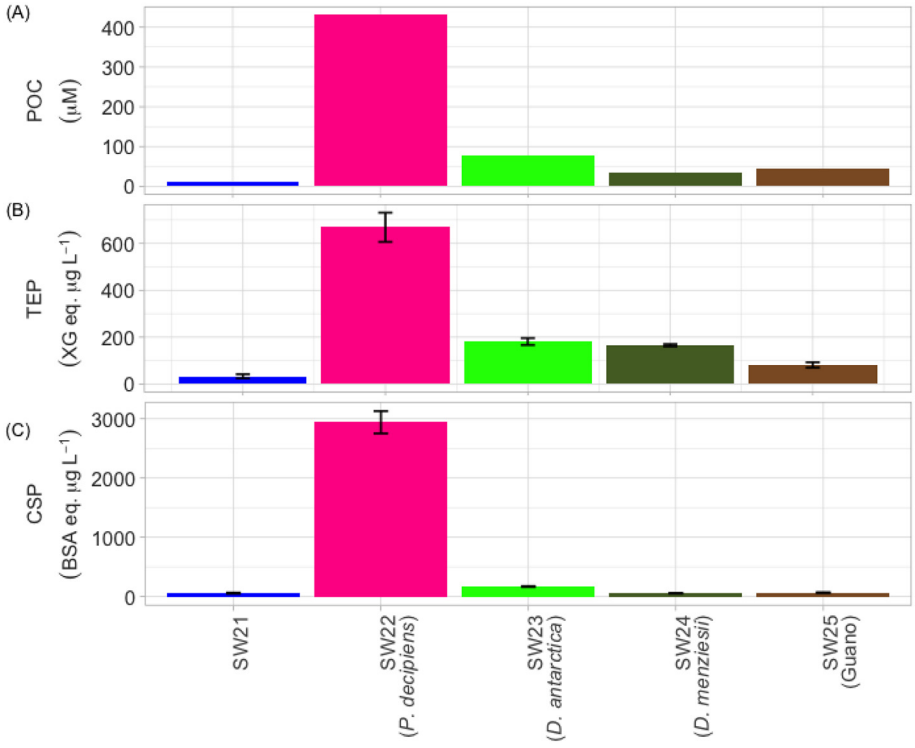

Fig. 5. (a) Particulate organic carbon (POC) and (b) TEP and (c) CSP measurements for the PI-ICE leaching material aerosol chamber experiments.

in the range 270–280 nm, indicative of absorbance of aromatic amino acids tryptophan (max 280 nm) and tyrosine (max 275 nm). They also show a slight shoulder in the MAAs region although very low. The absorbance spectrum of SW25, which was enriched with penguin excrement, shows a very distinct and relatively narrow peak centred at ~290 nm. This spectral pattern is extremely similar to that produced by uric acid, with the same maximum at 290 nm, whose absorbance can be used to determine the concentration of this substance in water. This similarity was not surprising, as seabird guano contains very high concentrations of uric acid, comprising ~80% of its nitrogen content by mass. Assuming all absorbance at 290 nm is due to uric acid, we estimate its concentration to be of 22 ± 2 μmol/L, which would account for about 80% of the dissolved organic nitrogen of the guano leachate experiment.

3.3.3. Particulate and dissolved sugars

The ambient seawater sample SW21 showed among the lowest concentrations of dissolved free carbohydrates (DFCHO, 1.1 μg L^{-1}), dissolved combined carbohydrates (DCCHO, 18.9 μg L^{-1}) and particulate combined carbohydrates (PCCHO, 27.3 μg L^{-1}) in comparison to the other ambient Surface Micro Layer (SML) and bulk water samples of this campaign (SW/SML1-SW/SML21, DFCHO: 1.0–17 μg L^{-1}, DCCHO: 14–294 μg L^{-1}, PCCHO: 13–248 μg L^{-1}, Zeppenfeld et al., 2021). All other water with leaching material, as expected, presented higher amount of sugars relative to SW21.

The sample from SW22 – which strongly suppressed primary aerosol formation – had the highest concentrations of carbohydrates. Surprisingly, the majority of carbohydrate was strongly dominated by DCCHO (18,064 μg L^{-1}) and only to a minor extent by PCCHO (973 μg L^{-1}). This makes a DCCHO:PCCHO ratio of 18.6 for *Palmaria decipiens*, much higher than for the ambient sample waters (SW1–SW21, Zeppenfeld et al., 2021, about 0.2–2.0). Within DCCHO, $xylose_{DCCHO}$ was by far the most abundant sugar (84.4 wt%), followed by $galactose_{DCCHO}$ (6 wt%) and $galacturonic\ acid_{DCCHO}$ (5 wt%). Surprisingly, $glucose_{DCCHO}$ (1.9 wt%) only contributed a minor part to DCCHO. This is unusual, since glucose is the most abundant monosaccharide in marine polysaccharides (about 20–90%). Interestingly, $xylose_{PCCHO}$ did not dominate PCCHO composition. Our results are consistent with the literature, given that *Palmaria* species are known to contain a high amount of water-soluble xylan polysaccharides as part of their cell wall (Hsieh et al., 2019; Usov, 2011). Xylans are known to stabilize protein foams, hence one possible explanation for the aerosol particle suppression is the formation and stabilization of foam, supporting previous studies reporting that sea foam forms from surface-active DOC attenuating laboratory primary sea spray generation (Keene et al., 2007). Contrary to sample SW22, the brown algae and guano leaching organic material of the remaining experiments (SW23, SW24, SW25) did not reveal any particular trend of the dissolved and particulate sugars.

3.4. Linking ocean-atmosphere variables

When looking at all the ocean-atmosphere variables presented, some conclusions can be drawn. The TEP/POC, CSP/POC and the CSP/TEP ratios are interesting. *Palmaria decipiens* SW22 had the lowest TEP/POC ratio, the lowest CSP/POC ratio and the highest CSP/TEP ratio, suggesting that proteic material may be responsible for the suppression of the aerosol production observed in the SW22 leaching material sample. However, given that SW22 had the lowest CSP/POC and TEP/POC ratio, it seems that the suppression of aerosol production observed is not caused by gel-like particles but other OM components.

We found that *Desmarestia antarctica* SW23 exhibited the highest viral abundances. The high viral abundance may determine more bacterial and/or eukaryote cell mortality, thus creating more organic material susceptible for aerosolisation. In other words, the interaction of sea ice viruses with prokaryotes and protists could liberate organic material to the water column, promoting the growth of other prokaryotes (viral loop) and stimulating their grazing by higher trophic levels (microbial loop and microbial food webs) (Boras et al., 2010; Maranger et al., 2015) and contributing to the overall biogeochemical cycles. Considering all treatments (three macroalgae leachate and guano additions), SW22 (*Palmaria decipiens*) and SW23 (with leachate of *Desmarestia antarctica*) showed the highest bacterial abundance. Moreover, we found that SW23 contained a high amount of HNF and also a high amount of viruses. This fact is probably due to the presence of OM which enhances bacterial growth and the subsequent dual

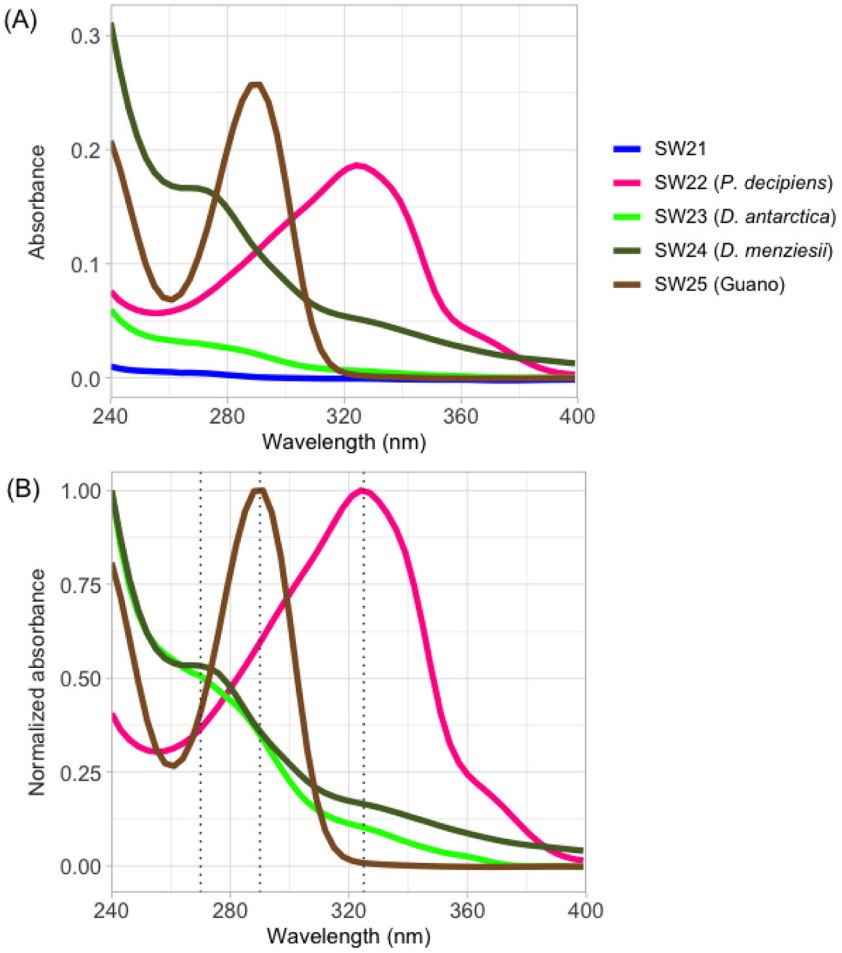

Fig. 6. Absolute absorbance of SW21 to SW25 (a) and normalized absorbance spectra of enriched samples (SW22 to SW25) (b). Dashed lines in (b) show the location of the main spectral features identified in mixes: shoulder at 270 nm (indicative of aromatic amino acids) and peaks at 290 nm (uric acid) and at 325 nm (mycosporine like amino acids).

effect: high prey availability for HNF proliferation and host to be lysed by viruses. This double mortality process will produce, in turn, new dissolved OM to be used again for bacteria. The highest HNF concentrations and maximum increment is seen for the 2–5 μm size fraction. Indeed, Dall'Osto et al. (2022) also found that HNF in melted sea ice samples was a relevant microbial component favouring sea spray aerosol production using a similar experimental setup and design. To our knowledge, the first SSA chamber experiments carried out with Antarctic melted sea ice were presented by Dall'Osto et al. (2017). Using three melted sea ice samples, it was suggested that SSA production cannot be link with the amount of phytoplankton biomass found in the sea ice. By contrast, it was argued that the maturity and decay of the algal assemblage would enhance SSA particle concentrations. Our study continues in the same direction, demonstrating that the microbiota ecosystems may have an important influence upon sea spray aerosol production.

4. Implications and conclusions

The chemical composition and the biogenic origin of organic matter (OM) emitted from the ocean as gases and particles is an area of increasing atmospheric research because they influence marine atmospheric chemistry and cloud-relevant aerosols. One of the major challenges in understanding the dynamics of primary sea spray production is the role of biogenic organic matter (OM) from the surface ocean. A chemoselective transfer of OM from the ocean to the atmosphere is often observed, meaning that some organic compounds are transported to the atmosphere to a larger extent than others (Quinn et al., 2015; Miyazaki et al., 2018; Santander et al., 2021). Here, we have shown that OM have an effect on aerosol particle production rates, which in turn can influence cloud properties, and may therefore be important for the changing climate. Besides for the known - but still controversial - phenomenon of marine microbiota influencing aerosol production (Prather et al., 2013; Sellegri et al., 2021), we show that leaching material from different ecosystem components can also influence the aerosol production in coastal areas, adding complexity to the ocean-atmosphere interphase in the AP study area.

In spite of many years studying SSA production, our understanding of the effect of organic matter (OM) is still limited. So far, we do not have consistent findings on how different surfactant-like compounds influence the SSA. Earlier studies showed different chemical components in the water have dichotomous effects on aerosol particle production, either enhancing or suppressing it (Garrett, 1968). It is becoming evident that a large variety of organic compounds in the sea water affect in different poorly known ways the formation of foam - in particular the complex relationship between the bubbling time and the nature of different surfactants (Sellegri et al., 2006, 2021). For example, the presence or the absence of a layer of foam on the surface of the ocean can drastically modify not only the SSA chemical composition but also the CCN properties (King et al., 2012). Higher SSA production was found in sea water with oleic acid (Tyree et al., 2007) or marine biogenic exudate from diatoms (Fuentes et al., 2010). Recently, a study by Sellegri et al. (2021) reported that the formation of foam can be limited by fatty acids components. This results in bubbles living shorter times - the resulting thicker bubble films increase the production of SSA. The SSA production depends on the different solubility of the surfactants. Soluble surfactants stabilize sea surface bubble bursting allowing bubbles to persist at the surface longer. In other words, a soluble surfactant can make bubbles live longer (the so called foam stabilization

effect). This results in thinner bubble films, this result in smaller SSA production therefore lower SSA emitted in the atmosphere. By contrast, insoluble surfactants have this effect only with small concentrations (Modini et al., 2013; Long et al., 2014). Surfactants not only increase bubble stability, but they also tend to decrease the friction velocity at the sea surface microlayer, with a net decrease of the bubble formation rate due to the lower entrainment of air. The resulting contrasting effects make the relationship between SSA production and surfactants very complex.

Our results should be put in the context that - under a warming by 1–5 °C degrees scenario, the AP will have more days with temperature above 0 °C (Convey and Peck, 2019). Increasing ocean turbulence will make the circumpolar deep water (CDW) both warmer and shallower. This results in coastal margins taking heat, likely thinning, and receding marine margins or glaciers and ice caps. Exposed (sea ice free) terrestrial open areas are also expected to increase, all these severe changes cause consequent structural changes.

Our study region is heavily influenced by ice disturbance, and the impact of iceberg sour on benthic life is still poorly understood (Barnes and Souster, 2011; Barnes et al., 2014). All such changes may have an effect on different organic material released in the surface of the ocean and then released in the atmosphere via SSA. More interdisciplinary investigations studying the interaction of the ocean with the cryosphere and its atmosphere and their influencing polar marine ecosystems are needed.

Data availability statement

The raw data of the current manuscript are available by contacting the corresponding author.

CRediT authorship contribution statement

MDO conceived the study; MDO, EB and DV obtained funding. MCB provided biogeochemical measurements, MVP and SZ provided sugars data. RPMM and CA collected and identified the macroalgae. RMH and DCSB provided the SMPS instrument. MR and MP provided H-NMR analysis. MVP and SZ provided sugar data and provided samples for INP analysis to HW. Olivia Linke executed the INP measurements at the TROPOS cloud group ice-lab which HW evaluated. MDO, DV, AS, MCB, EB, DCSB took the measurements and participated to the PI-ICE field study. All authors: experiment execution, and revision, correction, and approval of final manuscript.

Funding

The study was further supported by the Spanish Ministry of Economy through project PI-ICE (no. CTM 2017–89117-R) and the Ramon y Cajal fellowship (no. RYC-2012-11922). This work acknowledges the 'Severo Ochoa Centre of Excellence' accreditation (CEX2019-000928-S). The National Centre for Atmospheric Science (NCAS) Birmingham group is funded by the UK Natural Environment Research Council. DOC was analyzed by Mara Abad (ICM-CSIC) and the POC was analyzed at the IIM-CSIC (Vigo). We gratefully acknowledge the funding by the Deutsche Forschungsgemeinschaft (DFG, German Research Foundation, Projektnummer 268020496–TRR 172) within the Transregional Collaborative Research Center "ArctiC Amplification: Climate Relevant Atmospheric and SurfaCe Processes, and Feedback Mechanisms (AC)3" in subproject B04.

Declaration of competing interest

The authors declare that they have no known competing financial interests or personal relationships that could have appeared to influence the work reported in this paper.

Appendix A. Supplementary data

Supplementary data to this article can be found online at https://doi.org/10.1016/j.scitotenv.2022.154772.

References

Abakumova, E.V., Yu, I., Parnikozab, C., Zhianskid, M., Yanevad, R., Lupacheve, A.V., Andreevf, M.P., Yu, D., Vlasova, Rianog, J., Jaramillog, N., 2021. Ornithogenic factor of soil formation in Antarctica: a review. Eurasian Soil Science 54 (4), 528–540.

Álvarez-Salgado, X.A., Miller, A.E.J., 1998. Simultaneous determination of dissolved organic carbon and total dissolved nitrogen in seawater by high temperature catalytic oxidation: conditions for accurate shipboard measurements. Mar. Chem. 62, 325–333.

Amsler, C.D., Iken, K., McClintock, J.B., Amsler, M.O., Peters, K.J., Hubbard, J.M., Furrow, F.B., Baker, B.J., 2005. Comprehensive evaluation of the palatability and chemical defenses of subtidal macroalgae from the Antarctic peninsula. Mar. Ecol. Prog. Ser. 294, 141–159.

Amsler, et al., 2008. Chapter in Amsler book algal chemical ecology. Springer, Algal Chemical Ecology.

Ankisetty, Sridevi, Nandiraju, Santhisree, Win, Hla, Park, Young Chul, Amsler, Charles D., McClintock, James B., Baker, Jill A., Diyabalanage, Thushara K., Pasaribu, Albert, Singh, Maya P., Maiese, William M., Walsh, Rosa D., Zaworotko, Michael J., Baker, Bill J., 2004. Chemical investigation of predator-deterred macroalgae from the Antarctic peninsula. J. Nat. Prod. 67 (8), 1295–1302.

Barnes, D.K.A., Souster, T., 2011. Reduced survival of Antarctic benthos linked to climate-induced iceberg scouring. Nat. Clim. Chang. 1, 1–4. https://doi.org/10.1038/nclimate1232.

Benites Guardia, C.R., 2019. Actividad antibacteriana de macroalgas antárticas (Himantothallus grandifolius y Desmarestia confervoides) frente a cepas de Yersinia ruckeri, aisladas de trucha arco iris (Oncorhynchus mykiss).

Boersma, P.D., 2008. Penguins as marine sentinels. Bioscience 58 (7), 597–607.

Bonilla-Findji, O., Herndl, G.J., Gattuso, J.P., Weinbauer, M.G., 2009. Viral and flagellate control of prokaryotic production and community structure in offshore Mediterranean waters. Appl. Environ. Microbiol. 75, 4801–4812. https://doi.org/10.1128/AEM.01376-08.

Boras, J.A., Sala, M.M., Arrieta, J.M., Sa, E.L., Felipe, J., Agustí, S., Duarte, C.M., Vaqué, D., 2010. Effect of ice melting on bacterial carbon fluxes channelled by viruses and protists in the Arctic Ocean. Pol Biol 33, 1695–1707.

Brean, J., Dall'Osto, M., Simó, R., Shi, Z., Beddows, D.C.S., Harrison, R.M., 2021. Open Ocean and coastal new particle formation from sulfuric acid and amines around the Antarctic peninsula. Nat. Geosci. 14, 383–388. https://doi.org/10.1038/s41561-021-00751-y.

Brussaard, C.P., 2004. Optimization of procedures for counting viruses by flow cytometry. Appl. Environ. Microbiol. 70, 1506–1513.

Campana, G.L., Zacher, K., Momo, F.R., Deregibus, D., Debandi, J.I., Ferreyra, G.A., Ferrario, M.E., Wiencke, C., Quartino, M.L., 2020. Successional processes in Antarctic Benthic algae. Antarctic Seaweeds. Springer International Publishing, pp. 241–264. https://doi.org/10.1007/978-3-030-39448-6_12.

Carreto, J.I., Carignan, M.O., Montoya, N.G.A., 2005. High-resolution reverse-phase liquid chromatography method for the analysis of mycosporine-like amino acids (MAAs) in marine organisms. Mar. Biol. 146, 237–252. https://doi.org/10.1007/s00227-004-1447-y.

Carslaw, K.S., Lee, L.A., Reddington, C.L., Pringle, K.J., Rap, A., Forster, P.M., Mann, G.W., Spracklen, D.V., Woodhouse, M.T., Regayre, L.A., Pierce, J.R., 2013. Large contribution ofnatural aerosols to uncertainty in indirect forcing. Nature 503, 67–71. https://doi.org/10.1038/nature12674, Chen 2009.

Chubb, T., et al., 2016. Observations of high droplet number concentrations in Southern Ocean boundary layer clouds. Atmos. Chem. Phys. 16, 971–987. https://doi.org/10.5194/acp-16-971-2016.

Cisternas-Novoa, C., Lee, C., Engel, A., 2014. A semi-quantitative spectrophotometric, dye-binding assay for determination of coomassie blue stainable particles. Limnol. Oceanogr. Methods 12 (AUG), 604–616. https://doi.org/10.4319/lom.2014.12.604.

Clark, G.F., Raymond, B., Riddle, M.J., Stark, J.S., Johnston, E.L., 2015. Vulnerability of Antarctic shallow invertebrate-dominated ecosystems. Austral Ecol. 40, 482–491. https://doi.org/10.1111/aec.12237.

Clark, G.F., Stark, J.S., Palmer, A.S., Riddle, M.J., Johnston, E.L., 2017. The roles of sea-ice, light and sedimentation in structuring shallow Antarctic benthic communities. PLoS ONE 12, e0168391. https://doi.org/10.1371/journal.pone.0168391.

Clarke, A., Murphy, E.J., Meredith, M.P., King, J.C., Peck, L.S., Barnes, D.K., et al., 2007. Climate change and the marine ecosystem of the western Antarctic peninsula. Philos. Trans. R. Soc. B Biol. Sci. 362, 149–166. https://doi.org/10.1098/rstb.2006.1958.

Cochran, R.E., Ryder, O.S., Grassian, V.H., Prather, K.A., 2017. Sea spray aerosol: the chemical link between the oceans, atmosphere, and climate. Acc. Chem. Res. 50 (3), 599–604. https://doi.org/10.1021/acs.accounts.6b00603.

Convey, Peck, 2019. Antarctic environmental change and biological response. Sci. Adv. 5 (11), eaaz0888. https://doi.org/10.1126/sciadv.aaz0888 2019.

Corbisier, T.N., Petti, M.A.V., Skowronski, R.S.P., Brito, T.A.S., 2004. Trophic relationships in the nearshore zone of Martel inlet (King George Island, Antarctica): delta C-13 stable isotope analysis. Polar Biol. 27, 75–82.

Cunliffe, M., Engel, A., Frka, S., Gasparovic, B., Guitart, C., Murreell, J.C., Salter, M., Stolle, C., 2013. Sea surface microlayers: a unified physicochemical and biological perspective of the air-ocean interface. Prog. Oceanogr. 1109, 104–116.

Dall'Osto, M., Ovadnevaite, J., Paglione, M., Beddows, D.C.S., Ceburnis, D., Cree, C., Cortes, P., Zamanillo, M., Nunes, S.O., Perez, G.L., Ortega-Retuerta, E., Emelianov, M., Vaque, D., Marrase, C., Estrada, M., Sala, M.M., Vidal, M., Fitzsimons, M.F., Beale, R., Airs, R., Rinaldi, M., Decesari, S., Facchini, M.C., Harrison, R.M., O'Dowd, C., Simo, R., 2017. Antarctic Sea ice region as a source of biogenic organic nitrogen in aerosols. Sci. Rep. 7, 6047. https://doi.org/10.1038/s41598-017-06188-x.

Dall'Osto, M., Vaque, D., Sotomayor, Ana, Brufau, Miguel Cabrera, Estrada, Marta, Buchaca, Teresa, Soler, Montserrat, Nunes, Sdena, Zeppenfeld, Sebastian, Pinxteren, Manuela Van, Herrmann, Hartmut, Wex, Heike, Rinaldi, Matteo, Paglione, Marco, Beddows, David, Harrison, Roy M., Berdalet, Elisa, 2022. Sea ice microbiota in the Antarctic Peninsula modulates cloud-relevant sea spray aerosol production, under review. Frontiers in Marine Science section Marine Biogeochemistry In press.

Decesari, S., Facchini, M.C., Fuzzi, S., Tagliavini, E., 2000. Characterization of water-soluble organic compounds in atmospheric aerosol: a new approach. J. Geophys. Res. 105, 1481–1489.

Decesari, S., Paglione, M., Rinaldi, M., Dall'Osto, M., Simó, R., Zanca, N., Volpi, F., Facchini, M.C., Hoffmann, T., Götz, S., Kampf, C.J., O'Dowd, C., Ceburnis, D., Ovadnevaite, J., Tagliavini, E., 2020. Shipborne measurements of Antarctic submicron organic aerosols: an NMR perspective linking multiple sources and bioregions. Atmos. Chem. Phys. 20, 4193–4207. https://doi.org/10.5194/acp-20-4193-2020.

DKA, Barnes, Fenton, M., Cordingley, A., 2014. Climate-linked iceberg activity massively reduces spatial competition in Antarctic shallow waters. Curr Biol 24 (12), R553–R554. https://doi.org/10.1016/j.cub.2014.04.040.

Dos Santos, G.S., Rangel, K.C., Teixeira, T.R., Gaspar, L.R., Abreu-Filho, P.G., Pereira, L.M., Yatsuda, A.P., Gallon, M.E., Gobbo-Neto, L., da Costa Clementino, L., Graminha, M.A.S., Jordão, L.G., Pohlit, A.M., Colepicolo-Neto, P., Debonsi, H.M., 2020. GC-MS analysis, bioactivity-based molecular networking and antiparasitic potential of the Antarctic alga Desmarestia Antarctica. Planta Med. Int. Open 07 (03), e122–e132. https://doi.org/10.1055/a-1219-2207.

Edler, L., Elbrächter, M., 2005. The Utermöhl method for quantitative phytoplankton analysis. In: Karlson, B., Cusack, C., Bresnan, E. (Eds.), Intergovernmental Oceanographic Commission of ©UNESCO. 2010. Microscopic and Molecular Methods for Quantitative Phytoplankton Analysis. UNESCO, Paris (IOC Manuals and Guides, no. 55.) (IOC/2010/MG/55) 110 pages.

Engel, A., Bange, H.W., Cunliffe, M., Burrows, S.M., Friedrichs, G., et al., 2017. The ocean's vital skin: toward an integrated understanding of the sea surfacemicrolayer. Front. Mar. Sci. 4, 165. https://doi.org/10.3389/fmars.2017.00165.

Engel, A., Endres, S., Galgani, L., Schartau, M., 2020. Marvelous marine microgels: on the distribution and impact of gel-like particles in the oceanic water-column. Front. Mar. Sci. 7, 405. https://doi.org/10.3389/fmars.2020.00405.

Evans, C., Pearce, I., Brussaard, C.P.D., 2009. Viral-mediated lysis of microbes and carbon release in the sub-Antarctic and polar frontal zones of the Australian southern ocean. Environ. Microbiol. 11, 2924–2934.

Fossum, K.N., Ovadnevaite, J., Ceburnis, D., Dall'Osto, M., Marullo, S., Bellacicco, M., Simó, R., Liu, D., Flynn, M., Zuend, A., ODowd, C., 2017. Summertime primary and secondary contributions to southern ocean cloud condensation nuclei. Sci. Rep. 8 (11), 13844. https://doi.org/10.1038/s41598-018-32047-4.

Fraser, C.I., Morrison, A., Olmedo Rojas, P., 2020. Biogeographic processes influencing Antarctic and sub-Antarctic seaweeds. Antarctic Seaweeds. Springer International Publishing, pp. 43–57 https://doi.org/10.1007/978-3-030-39448-6_3.

Fuentes, E., Coe, H., Green, D., de Leeuw, G., McFiggans, G., 2010. On the impacts of phytoplankton-derived organic matter on the properties of the primary marine aerosol – part 1: source fluxes. Atmos. Chem. Phys. 10, 9295–9317. https://doi.org/10.5194/acp-10-9295-2010.

Gagnon, P., St-Hilaire-Gravel, Louis Vincent, Himmelman, J.H., Johnson, L.E., 2006. Organismal defenses versus environmentally mediated protection from herbivores: unraveling the puzzling case of Desmarestia viridis (Phaeophyta). J. Exp. Mar. Biol. Ecol. 334 (1), 10–19. https://doi.org/10.1016/J.JEMBE.2006.01.012.

Gagnon, P., Blain, C., Vad, J., 2012. Living within constraints: irreversible chemical build-up and seasonal temperature-mediated die-off in a highly acidic (H2SO4) annual seaweed (Desmarestia viridis). Marine Biology 160 (2), 439–451. https://doi.org/10.1007/S00227-012-2101-8 2012 160:2.

Gallardo, T., Pérez-Ruzafa, I.M., Flores-Moya, A., Conde, F., 1999. New Collections of Benthic Marine Algae from Livingston and Deception Islands (South Shetland Islands) and Trinity Island (Bransfield Strait) Antarctica. Botanica Marina 42 (1). https://doi.org/10.1515/BOT.1999.009.

Gantt, B., Meskhidze, N., 2013. The physical and chemical characteristics of marine primary organic aerosol: a review. Atmos. Chem. Phys. 13, 3979–3996. https://doi.org/10.5194/acp-13-3979-2013.

Garcia-Borboroglu, P., Boersma, P.D., 2013. Penguins. Natural History and Conservation. University of Washington Press.

Garrett, W.D., 1968. Influence of monomolecular surface films on production of condensation nuclei from bubbled sea water. J. Geophys. Res. 73, 5145–5150. https://doi.org/10.1029/JB073 i016p 05145.

Gasol, J.M., Del Giorgio, P.A., 2000. Using flow cytometry for counting natural planktonic bacteria and understanding the structure of planktonic bacterial communities. Sci. Mar. 64 (2), 197–224.

Gasol, J.M., Zweifel, U.L., Peters, F., Fuhrman, J.A., Hagström, Å., 1999. Significance of size and nucleic acid content heterogeneity as measured by flow cytometry in natural planktonic bacteria. Appl. Environ. Microbiol. 65, 4475–4483. https://doi.org/10.1128/AEM.65.10.4475-4483.1999.

Gómez, I., Huovinen, P., 2020. Antarctic seaweeds: biogeography, adaptation, and ecosystem services. In: Gómez, I., Huovinen, P. (Eds.), Antarctic Seaweeds. Springer, pp. 3–20 https://doi.org/10.1007/978-3-030-39448-6_1.

Gómez, I., Wulff, A., Roleda, M.Y., Huovinen, P., Karsten, U., Quartino, M.L., Dunton, K., Wiencke, C., 2009. Light and temperature demands of marine benthic microalgae and seaweeds in polar regions. Botanica Marina 52 (6), 593–608. https://doi.org/10.1515/BOT.2009.073 Walter de Gruyter.

Gong, X., Wex, H., van Pinxteren, M., Triesch, N., Fomba, K.W., Lubitz, J., Stolle, C., Robinson, B., Müller, T., Herrmann, H., Stratmann, F., 2020. Characterization of aerosol particles at Cape Verde close to sea and cloud level heights - part 2: ice nucleating particles in air, cloud and seawater. Atmos. Chem. Phys. 20, 1451–1468. https://doi.org/10.5194/acp-20-1451-2020.

Hartmann, M., Gong, X., Kecorius, S., van Pinxteren, M., Vogl, T., Welti, A., Wex, H., Zeppenfeld, S., Herrmann, H., Wiedensohler, A., Stratmann, F., 2021. Terrestrial or marine? – indications towards the origin of ice nucleating particles during melt season in the european Arctic up to 83.7°N. Atmos. Chem. Phys. 21, 11613–11636. https://doi.org/10.5194/acp-21-11613-2021.

Holm-Hansen, O., Lorenzen, C.J., Holmes, R.W., Strickland, J.D.H., 1965. Fluorometric determination of chlorophyll. ICES J. Mar. Sci. 30 (1), 3–15. https://doi.org/10.1093/icesjms/30.1.3.

Hsieh, Y.S.Y., Harris, P.J., Xylans, 2019. of Red and Green Algae: What Is Known about Their Structures and How They Are Synthesised?. 11, p. 354. https://doi.org/10.3390/polym11020354

Iken, K., Amsler, Charles D., Amsler, Margaret O., McClintock, James B., Baker, Bill J., 2009. Field studies on deterrent properties of phlorotannins in Antarctic brown algae. Bot. Mar. 52, 547–557. https://doi.org/10.1515/BOT.2009.071.

Iken, K., Amsler, C.D., Amsler, M.O., McClintock, J.B., Baker, B.J., 2011. Field studies on deterrent properties of phlorotannins in Antarctic brown algae. In: Wiencke, C. (Ed.), Biology of Polar Benthic Algae. Walter de Gruyter, pp. 121–140.

Keene, W.C., et al., 2007. Chemical and physical characteristics of nascent aerosols produced by bursting bubbles at a model air-sea interface. J. Geophys. Res. 112, D21202. https://doi.org/10.1029/2007JD008464.

King, S.M., Butcher, A.C., Rosenoern, T., Coz, E., Lieke, K.I., de Leeuw, G., Douglas Nilsson, E., Bilde, M., 2012. Investigating primary marine aerosol properties: CCN activity of seasalt and mixed inorganic-organic particles. Environ. Sci. Technol. 49 (19), 10405–10412.

Lagger, C., Nime, M., Torre, L., Servetto, N., Tatián, M., Sahade, R., 2018. Climate change, glacier retreat and a new ice-free island offer new insights on Antarctic benthic responses. Ecography 41 (4), 579–591. https://doi.org/10.1111/ecog.03018.

Lewis, S.L., Saliba, G., Russell, L.M., Quinn, P.K., Bates, T.S., Behrenfeld, M.J., 2021. Seasonal differences in submicron marine aerosol particle organic composition in the North Atlantic. Front. Mar. Sci. 8, 720208. https://doi.org/10.3389/fmars.2021.720208.

Li, Z., Niu, F., Fan, J., Liu, Y., Rosenfeld, D., Ding, Y., 2011. Long-term impacts of aerosols on the vertical development of clouds and precipitation. Nat. Geosci. 4, 888–894.

Long, M.S., Keene, W.C., Kieber, D.J., Frossard, A.A., Russell, L.M., Maben, J.R., et al., 2014. Light-enhanced primary marine aerosol production from biologically productive seawater. Geophys. Res. Lett. 41 (7), 2661–2670. https://doi.org/10.1002/2014GL059436.

Mansour, K., Decesari, S., Facchini, M.C., Belosi, F., Paglione, M., Sandrini, S., et al., 2020. Linking marine biological activity to aerosol chemical composition and cloud-relevant properties over the North Atlantic Ocean. J. Geophys. Res.-Atmos. 125, e2019JD032246. https://doi.org/10.1029/2019JD032246.

Maranger, R., Vaqué, D., Nguyen, D., Hébert, M.P., Lara, E., 2015. Pan-Arctic patterns of planktonic heterotrophic microbial abundance and processes: controlling factors and potential impacts of warming. Progr. Oceanogr. 139, 221–232.

Marquardt, J., Hanelt, D., 2004. Carotenoid composition of Delesseria lancifolia and other marine red algae from polar and temperate habitats. Eur. J. Phycol. 39 (3), 285–292. https://doi.org/10.1080/09670260410001712572.

Matsuhiro, B., Urzúa, C.C., 1996. The acidic polysaccharide from Palmaria decipiens (Palmariales, Rhodophyta). Hydrobiologia 326, 491–495. https://doi.org/10.1007/BF00047850.

McCluskey, C.S., Hill, T.C.J., Humphries, R.S., Rauker, A.M., Moreau, S., Strutton, P.G., Chambers, S.D., Williams, A.G., McRobert, I., Ward, J., Keywood, M.D., Harnwell, J., Ponsonby, W., Loh, Z.M., Krummel, P.B., Protat, A., Kreidenweis, S.M., DeMott, P.J., 2018. Observations of ice nucleating particles over Southern Ocean waters. Geophys. Res. Lett. 45 (21), 11989–11997. https://doi.org/10.1029/2018gl079981.

Medina-Pérez, N.-I., Dall'Osto, M., Decesari, S., Paglione, M., Moyano, E., Berdalet, E., 2020. Aerosol toxins emitted by harmful algal blooms susceptible to complex air-sea interactions. Environ. Sci. Technol. 55 (1), 469–477. https://doi.org/10.1021/acs.est.0c05795.

Mender-Deuer, S., Lessard, E.J., 2000. Carbon to volume relationships for dinoflagellates, diatoms, and other protist plankton. Limnol. Oceanogr. 45 (3), 569–579.

Miyazaki, Y., Yamashita, Y., Kawana, K., Tachibana, E., Kagami, S., Mochida, M., Suzuki, K., Nishioka, J., 2018. Chemical transfer of dissolved organic matter from surface seawater to sea spray water-soluble organic aerosol in the marine atmosphere. Sci. Rep. 8 (1), 1–10. https://doi.org/10.1038/s41598-018-32864-7.

Modini, R.L., Russell, L.M., Deane, G.B., Stokes, M.D., 2013. Effect of soluble surfactant on bubble persistence and bubble-produced aerosol particles. J. Geophys. Res. 118, 1388–1400. https://doi.org/10.1002/jgrd.50186.

Moran, X.A.G., Lopez-Urrutia, A., Calvo-Dıaz, A., Li, W.K.W., 2010. Increasing importance of small phytoplankton in a warmer ocean. Global Change Biology 16, 1137–1144.

Oliveira, M.C., Pellizzari, F., Medeiros, A.S., Yokoya, N.S., 2020. Diversity of Antarctic seaweeds. In: Gómez, I., Huovinen, P. (Eds.), Antarctic Seaweeds. Springer, pp. 23–42 https://doi.org/10.1007/978-3-030-39448-6_2.

Otero, X.L., De La Peña-Lastra, S., Pérez-Alberti, A., Ferreira, T.O., Huerta-Diaz, M.A., 2018. Seabird colonies as important global drivers in the nitrogen and phosphorus cycles. Nat. Commun. 9 (1). https://doi.org/10.1038/s41467-017-02446-8.

Park, J., Dall'Osto, M., Park, K., Park, J., Hwang, C.Y., Jang, G., Gim, Y., Kang, S., Kim, J.-H., Park, K.-T., 2019. Artic primary aerosol production strongly influenced by riverine organic matter. Environ. Sci. Technol. 53, 8621–8630.

Park, J., Dall'Osto, M., Park, K., Gim, Y., Kang, H.J., Jang, E., Park, K.-T., Park, M., Yum, S.S., Jung, J., Lee, B.Y., Yoon, Y.J., 2020. Shipborne observations reveal contrasting Arctic marine, Arctic terrestrial and Pacific marine aerosol properties. Atmos. Chem. Phys. Discuss. 20, 5573–5590.

Passow, U., Alldredge, A.L., 1995. A dye-binding assay for the spectrophotometric measurement of transparent exopolymer particles (TEP). Limnol. Oceanogr. 40, 1326–1335. https://doi.org/10.4319/lo.1995.40.7.1326.

Peck, L.S., 2018. Antarctic marine biodiversity: adaptations, environments and responses to change. Oceanogr. Mar. Biol. Annu. Rev. 56, 105–236.

Pelletreau, K., Muller-Parker, G., 2002. Sulfuric acid in the phaeophyte alga Desmarestia munda deters feeding by the sea urchin Strongylocentrotus droebachiensis. Marine Biology 141 (1), 1–9. https://doi.org/10.1007/S00227-002-0809-6 2002 141:1.

Pellizzari, F., Silva, M.C., Silva, E.M., Medeiros, A., Oliveira, M.C., Yokoya, N.S., Pupo, D., Rosa, L.H., Colepicolo, P., 2017. Diversity and spatial distribution of seaweeds in the South Shetland Islands, Antarctica: an updated database for environmental monitoring under climate change scenarios. Polar Biol. 40 (8), 1671–1685. https://doi.org/10.1007/s00300-017-2092-5.

Prather, K.A., Bertram, T.H., Grassian, V.H., Deane, G.B., Stokes, M.D., Demott, P.J., et al., 2013. Bringing the ocean into the laboratory to probe the chemical complexity of sea spray aerosol. Proc. Natl. Acad. Sci. U. S. A. 110 (19), 7550–7555. https://doi.org/10.1073/pnas.1300262110.

Quartino, M.L., Zaixso, H.E., Boraso de Zaixso, A.L., 2005. Biological and environmental characterization of marine macroalgal assemblages in potter cove, South Shetland IslandsAntarctica. Bot. Mar. 48, 187–197.

Quartino, M.L., Deregibus, D., Campana, G.L., Latorre, G.E.J., Momo, F.R., 2013. Evidence of macroalgal colonization on newly ice-free areas following glacial retreat in potter cove (South Shetland Islands)Antarctica. PLoS ONE 8 (3), 8–15. https://doi.org/10.1371/journal.pone.0058223.

Quartino, M.L., Saravia, L.A., Campana, G.L., Deregibus, D., Matula, C.V., Boraso, A.L., Momo, F.R., 2020. Production and biomass of seaweeds in newly ice-free areas: implications for coastal processes in a changing Antarctic environment. Springer International Publishing, pp. 155–171 https://doi.org/10.1007/978-3-030-39448-6_8 Antarctic Seaweeds.

Quinn, P.K., Bates, T.S., 2011. The case against climate regulation via oceanic phytoplankton sulphur emissions. Nature 480 (7375), 51–56. https://doi.org/10.1038/nature10580.

Quinn, P.K., Collins, D.B., Grassian, V.H., Prather, K.A., Bates, T.S., 2015. Chemistry and related properties of freshly emitted sea spray aerosol. Chem. Rev. 115 (10), 4383–4399. https://doi.org/10.1021/cr500713g.

Rahlff, J., Stolle, C., Giebel, H.-A., Mustafa, N.I.H., Wurl, O., Herlemann, D.P.R., 2021. Sea foams are ephemeral hotspots distinctive bacteria communities contrasting sea-surface microlayer and underlying surface water. FEMS Microbiol. Ecol. 97 (fiab035). https://doi.org/10.1093/femsec/fiab035.

Rinaldi, M., Paglione, M., Decesari, S., Harrison, R.M., Beddows, D.C.S., Ovadnevaite, J., Ceburnis, D., O'Dowd, C., Simó, R., Dall'Osto, M., 2020. Contribution of water-soluble organic matter from multiple marine geographic eco-regions to aerosols around Antarctica. Environ. Sci. Technol. 54, 7807–7817. https://doi.org/10.1021/acs.est.0c00695.

Ronowicz, M., Peña Cantero, A.L., Mercado Casares, B., Kuklinski, P., Soto Àngel, J.J., 2019. Assessing patterns of diversity, bathymetry and distribution at the poles using hydrozoa (Cnidaria) as a model group. Hydrobiologia 833, 25–51. https://doi.org/10.1007/s10750-018-3876-5.

Rovelli, L., Attard, K.M., Cárdenas, C.A., Glud, R.N., 2019. Benthic primary production and respiration of shallow rocky habitats: a case study from South Bay (Doumer Island, Western Antarctic Peninsula). Polar Biol. 42 (8), 1459–1474. https://doi.org/10.1007/s00300-019-02533-0.

Santander, M.V., Mitts, B.A., Pendergraft, M.A., Dinasquet, J., Lee, C., Moore, A.N., Cancelada, L.B., Kimble, K.A., Malfatti, F., Prather, K.A., 2021. Tandem fluorescence measurements of organic matter and bacteria released in sea spray aerosols. Environ. Sci. Technol. 55 (8), 5171–5179. https://doi.org/10.1021/acs.est.0c05493.

Schofield, O., Saba, G., Coleman, K., Carvalho, F., Couto, N., Ducklow, H., Finkel, Z., Irwin, A., Kahl, A., Miles, T., Montes-Hugo, M., Stammerjohn, S., Waite, N., 2017. Decadal variability in coastal phytoplankton community composition in a changing West Antarctic peninsula. Deep-Sea Res. Pt. I 124, 42–54. https://doi.org/10.1016/j.dsr.2017.04.014.

Sellegri, K., Odowd, C.D., Yoon, Y.J., Jennings, S.G., Deleeuw, G., 2006. Surfactants and submicron sea spray generation. J. Geophys. Res. https://doi.org/10.1029/2005J D0066 58.

Sellegri, K., Nicosia, A., Freney, E., et al., 2021. Surface Ocean microbiota determine cloud precursors. Sci. Rep. 11, 281. https://doi.org/10.1038/s41598-020-78097-5.

Sieracki, M.E., Johnson, P.W., Sieburth, J.M., 1985. Detection, enumeration, and sizing of planktonic bacteria by image-analyzed epifluorescence microscopy. Appl. Environ. Microbiol. 49 (4), 799–810.

Stocker, T.F., Qin, D., Plattner, G.-K., Alexander, L.V., Allen, S.K., Bindoff, N.L., Bréon, F.-M., Church, J.A., Cubasch, U., Emori, S., Forster, P., Friedlingstein, P., Gillett, N., Gregory, J.M., Hartmann, D.L., Jansen, E., Kirtman, B., Knutti, R., Kumar, K.Krishna, Lemke, P., Marotzke, J., Masson-Delmotte, V., Meehl, G.A., Mokhov, I.I., Piao, S., Ramaswamy, V., Randall, D., Rhein, M., Rojas, M., Sabine, C., Shindell, D., Talley, L.D., Vaughan, D.G., Xie, S.-P., 2013. Technical summary. In: Stocker, T.F., Qin, D., Plattner, G.-K., Tignor, M., Allen, S.K., Doschung, J., Nauels, A., Xia, Y., Bex, V., Midgley, P.M. (Eds.), Climate Change 2013: The Physical Science Basis. Contribution of Working Group I to the Fifth Assessment Report of the Intergovernmental Panel on Climate Change. Cambridge University Press, pp. 33–115 https://doi.org/10.1017/CBO9781107415324.005.

Thomas, D.N., Dieckmann, G.S., 2003. Sea Ice. An Introduction to Its Physics, Chemistry, Biology and Geology. Blackwell, Great Britain.

Tyree, C.A., Hellion, V.M., Alexandrova, O.A., Allen, J.O., 2007. Foam droplets generated from natural and artificial seawaters. J. Geophys. Res. 112, D12204. https://doi.org/10.1029/2006J D0077 29.

Usov, A., 2011. Polysaccharides of the red algae. Adv. Carbohydr. Chem. Biochem. 65, 115–217. https://doi.org/10.1016/B978-0-12-385520-6.00004-2.

Vali, G., 1971. Quantitative evaluation of experimental results on heterogeneous freezing nucleation of supercooled liquids. J. Atmos. Sci. 28 (3), 402–409. https://doi.org/10.1175/1520-0469(1971)028<0402:qeoera>2.0.co;2.

Vaqué, D., Casamayor, E.O., Gasol, J.M., 2001. Dynamics of whole community bacterial production and grazing losses in seawater incubations as related to the changes in the proportions of bacteria with different DNA-content. Aquat. Microb. Ecol. 25, 163–177.

Vaqué, D., Boras, J.A., Arrieta, J.M., Agustí, S., Duarte, C.M., Sala, M.M., 2021. Enhanced viral activity in the surface microlayer of the Arctic and Antarctic oceans. Microorganisms 9, 317. https://doi.org/10.3390/microorganisms9020317.

Wiencke, C., Amsler, C.D., 2012. Seaweeds and Their Communities in Polar Regions. Springer, Berlin, Heidelberg, pp. 265–291. https://doi.org/10.1007/978-3-642-28451-9_13.

Wiencke, C., Clayton, M.N., 2002. Biology of Antarctic Seaweeds. A.R.G Gantner Verlag KG, Liechtenstein.

Wiencke, C., Clayton, M.N., Clayton, N.M., 2002. Antarctic seaweeds. In: Wägele, J.W. (Ed.) Synopses of the Antarctic Benthosvol. 9. Koeltz Botanical Books, p. (p. 239).

Wong, S.-K., Suzuki, S., Cui, Y., Kaneko, R., Kogure, K., Hamasaki, K., 2021. Sampling constraints and variability in the analysis of bacterial community structures in the sea surface microlayer. Front. Mar. Sci. 8, 696389. https://doi.org/10.3389/fmars.2021.696389.

Wurl, O., Ekau, W., Landing, W.M., Zappa, C.J., 2017. Sea surface microlayer in a changing ocean –a perspective. Elementa (Wash. D.C.) 5, 31. https://doi.org/10.1525/elementa.228.

Zeppenfeld, S., van Pinxteren, M., Engel, A., Herrmann, H., 2020. A Protocol for Quantifying Mono- and Polysaccharides in Seawater and Related Saline Matrices by Electro-dialysis (ED) – Combined With HPAEC-PAD. 16, pp. 817–830. https://doi.org/10.5194/os-16-817-2020.

Zeppenfeld, S., van Pinxteren, M., van Pinxteren, D., Wex, H., Berdalet, E., Vaqué, D., Dall'Osto, M., Herrmann, H., 2021. Aerosol marine primary carbohydrates and atmospheric transformation in the Western Antarctic Peninsula. ACS Earth Space Chem. 5, 1032–1047. https://doi.org/10.1021/acsearthspacechem.0c00351.

Zhu, Renbin, Wang, Qing, Ding, Wei, Wang, Can, Hou, Lijun, Ma, Dawei, 2014. Penguins significantly increased phosphine formation and phosphorus contribution in maritime Antarctic soils. Scientific Reports 4, 7055. https://doi.org/10.1038/srep07055 Walter de Gruyter.